Detailed Studies on the Beam Transfer Line from Linac to Low Energy Booster Synchrotron for the SSC

R. Bhandari, J. McGill, F. Wang and S. Penner

Superconducting Super Collider Laboratory*, 2550 Beckleymeade Avenue, Dallas, TX 75237, USA

Abstract

Ion optical and engineering aspects of the Linac to LEB transfer line [1] are described. This 210 m long line will transport a 600 MeV H^- beam between the two accelerators. Emittance growth expected at injection due to errors on various components in the line has been estimated. Some design details of the LEB injection girder are presented.

I. INTRODUCTION

A 600 MeV H^- Linac [2] is the first accelerator in the chain of four injectors for the Collider. It is presently under construction and scheduled to be operational by summer 1995. Simulation studies show that the linac beam emittance is expected to be 0.23 π mm-mrad, rms, normalized, in each transverse plane. In order to limit the emittance to 1 π mm-mrad at 20 TeV in the Collider, it is necessary to restrict the emittance growth at successive injection and acceleration stages. As per the overall emittance growth budget, final emittance after completion of the LEB injection cycle should not exceed 0.4 π mm-mrad. This growth results due to various injection errors and scattering in the carbon foil used for charge exchange injection. Several beam diagnostic elements have been provided on the line to meet the emittance growth requirements. Beam halos will be scraped and dumped on the absorbers in a controlled manner in order to minimize activation of the accelerator components and surroundings

II. STATUS AND DETAILS OF THE TRANSFER LINE

First half of this transfer line (figure 1a) is primarily a FODO array with 90° phase advance. It utilizes quadrupoles with 23 mm aperture diameter. These quadrupoles are identical to those used in the Coupled Cavity Linac (CCL), which accelerates the beam from 70 to 600 MeV. Two prototypes have been fabricated and field measured. The measured and calculated field properties compare very well. Industrial production of 106 quadrupoles will begin in the summer of this year. All these magnets have built-in steering coils which will be selectively energized. Four picture frame type steering magnets have been provided at the beginning of the line to align the CCL beam onto the optic axis with the help of four position monitors. The diagnostic elements e.g. position monitors, toroids, wire scanners etc. are the same as those on the CCL. Wire scanners will, primarily, be used to tune first four matching quadrupoles which are independently excited. We plan to use the least square fitting technique with deviations in

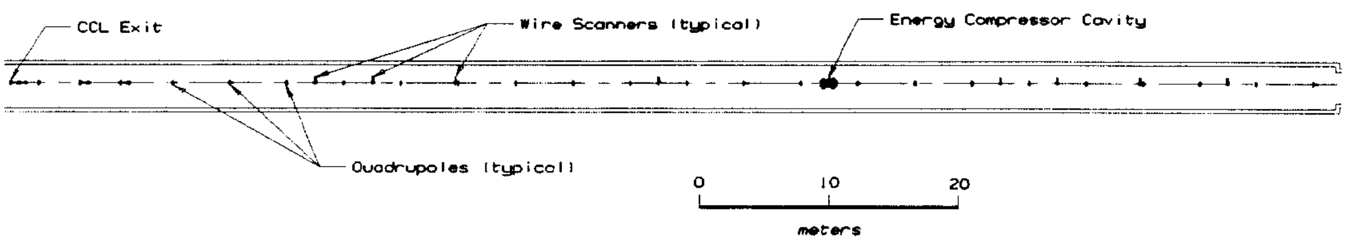

Figure 1a. First half of the Linac to LEB transfer line. Beam is transported by a FODO array over 80% of the length of this half.

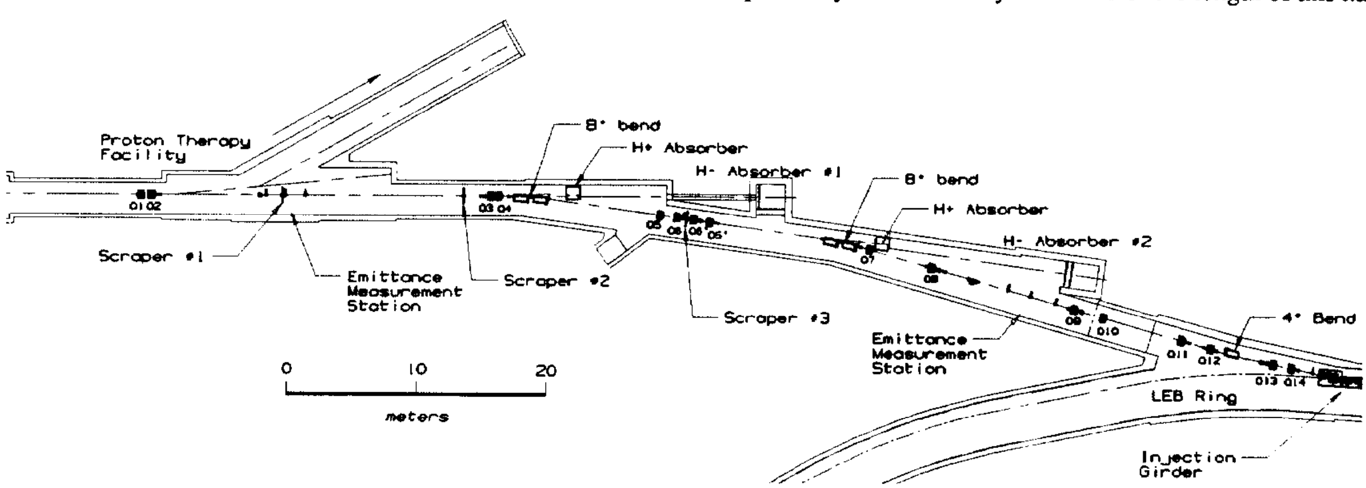

Figure 1b. Second half of the Linac to LEB transfer line. Q: Quadrupole magnets. Scrapers are about 500 $\mu g/cm^2$ thick carbon foils. Provision has been kept in the building to switch the beam toward a future proton therapy facility.

* Operated by the Universities Research Association, Inc. for the U.S. Department of Energy, under the Contract No. DE-AC35-89ER40486.

the beam sizes from matched values as dependent and quadrupole currents as independent variables. Nineteen quadrupoles, which actually form the FODO array, are energized using two power supplies. Last two quadrupoles on this half are also used for phase space matching. In order to improve the pumping efficiency, larger beam pipe sections (75 mm) have been provided between the quadrupoles which are 4.3 m apart. There will be one ion pump on each of these sections.

Second half of the transfer line (figure 1b) has larger cross section, in general. It uses quadrupoles with aperture diameter of 75 mm. Engineering drawings for these quadrupoles and the steering magnets have been prepared and industrial prototypes will be ready for measurements in July 1993. There are two 8^o and one 4^o bends on this line. Each 8^o bend consists of two 4^o dipole magnets 0.5 m apart. We are, therefore, building five identical 4^o dipoles, each being a 1 m long rectangular magnet. Maximum bending field has been restricted to 4 kG at 1 GeV to limit losses due to Lorentz stripping in the beamline to 0.1% [3]. Splitting the 8^o bends offers another advantage i.e. the scraped beam is diverted toward H^+ absorbers without experiencing strong edge defocussing effects. Dipole magnets have been designed to keep $\Delta B/B$ due to sextupole component below 1×10^{-4} at 1 cm from the central ray. This eliminates the need for sextupole magnets which were earlier provided to minimize the phase space distortion at dispersive location at the center of the achromat formed by two 8^o bends. A prototype dipole will be assembled in-house by September 1993. All the magnets are designed for operation upto 1 GeV energy.

Injection Girder

Figure 2 shows the injection girder assembly. Four identical bump magnets, excited by one power supply in series, will bump the circulating beam by 47.2 mm from the LEB axis during injection. Each bump has a magnetic length of 0.6 m. A 1.4 m long septum magnet separates the injected beam from the circulating beam. Figure 3 shows cross sections of the first bump and the septum magnets at their exit ends, and relative positions of the injected, bumped and circulating beams. An iron shield between the two magnets minimizes the magnetic field interaction. Bump magnets have a flattop time of 35 μs. While the rise time is not so critical, the fall time should be shortest possible (section III). Excitation waveform for the septum magnet is a 1.5 ms half sine wave. The magnets will be made using thin (0.05 mm) laminations in form of a tape wound core (figure 3). All these magnets have been designed to operate at 4 kG peak field at 1 GeV. Mechanical designs have been completed and the prototypes are expected to be supplied by industry in October 1993. Bump magnets have ceramic vacuum chambers to eliminate eddy current effects.

The H^- beam will be stripped to H^+, with 95 % efficiency, using a 200-250 $\mu g/cm^2$ thick carbon foil placed midway between bump 2 and bump 3 magnets [3]. Over 4% of the incoming beam will be converted into H^0 and the rest remains H^-. The H^0 beam travels undeflected to a beam stop at the exit of bump 4. The H^- beam, bent to the left by bump 3, comes out into the air through a thin window to fall on the same beam stop. Intensity of this beam will be monitored. Its unusual rise will indicate foil rupture. Two position monitors, downstream of bump 4, on the LEB ring will be used to align the injected beam. A foil positioning mechanism holds spare foils, and TV viewed flag, and changes them without breaking the vacuum.

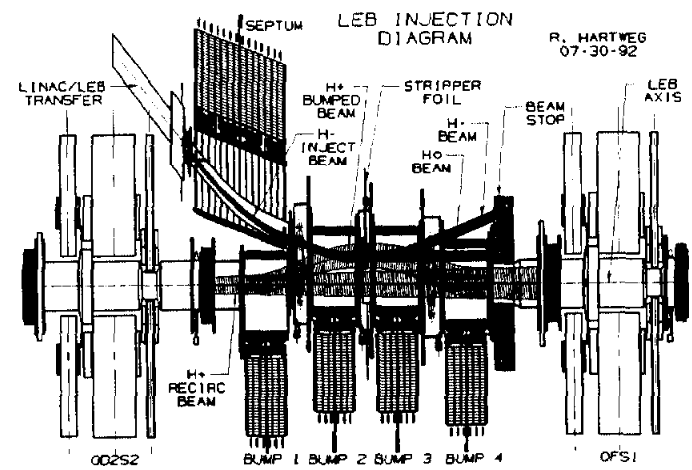

Figure 2. LEB injection girder assembly. Quadrupoles QD2S2 and QFS1 belong to the LEB lattice. Wire scanners between bumps 1 & 2 and bumps 3 & 4 will scan both injected and circulating beams. Vertical scale has been blown up for clarity.

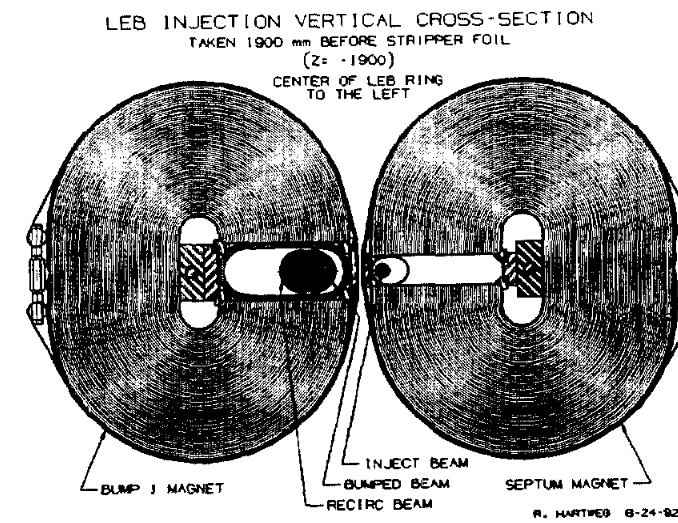

Figure 3. Cross section at the exit ends of the bump1 and the septum magnets.

Energy Compressor Cavity

No. of cells has been reduced to 11, from earlier 20, to keep phase shift for the RF drive low at the onset of the beam loading. At the same time, total power requirement was also kept low. Primary function of this cavity is to reduce energy spread of the beam. However, it also corrects for the energy jitter due to CCL instabilities. The energy correction is given by:

$$\Delta T_c = q \, . \, (E_0 T) L \, . \, \cos(\Delta\phi + \Delta\theta - \pi/2)$$

where, E_0T is the average accelerating gradient, L is cavity length, $\Delta\phi$ is phase difference between the ideal particle and a particle with energy error and $\Delta\theta$ is the RF phase fluctuation. Ideal particle undergoes no energy change if $\Delta\theta$=0.

Beam Scraping

Two scrapers, installed upstream of the first 8^o bend, will scrape particles which are very much off in position and angle in each transverse plane. Ray tracing calculations, using TURTLE, show that a majority of scraped particles (H^+) can be transported to the absorbers without hitting the beamline components. Similar results were obtained for the off momentum particles scraped at the center of the achromat. In both case, these particles do not enter the second 4° dipole of the 8° bends. Instead, they come out of the exit edge of the first 4° dipole and travel straight to the absorber.

Beam Steering

In the first half of the line, there are three beam alignment systems in each plane. Each system consists of two steerers and two position monitors. In the second half, a position monitor is provided near every quadrupole cluster and a steerer is placed upstream. Last two steerers in each plane allow near orthogonal control of position and angle at the injection point.

III. EMITTANCE GROWTH

Magnetic field instabilities, phase space and dispersion mismatches and scattering in the stripper foil are the major sources of emittance growth. We have used Sypher's formalism [4] to estimate emittance growth due to first two sources. In this formalism, time average distribution under the effect of the errors is calculated. By comparing it with the initial distribution, emittance dilution factor is obtained. Emittance growth (rms, normalized) due to dipole field instability is given by:

$$\Delta\varepsilon_n = 0.5\,\pi\,\beta_l\,(\Delta\alpha)^2(\beta\gamma)_{\text{Lorentz}}$$

where, β_l is the lattice beta function at the dipole and $\Delta\alpha$ is deviation in the bending angle due to field change. Normalized emittance growth values (rms) expected due to field instability in various dipole magnets are as follows:

Bump (Stability 0.1%) : 0.0153 π mm-mrad

Septum (Stability 0.04%) : 0.0082 π mm-mrad

D2 Dipole (Stability 0.01%): 0.0013 π mm-mrad

Since, all 4 magnets of the achromat are excited by one power supply in series, there is, ideally, no net effect due to field instability. The stability of this power supply is also 0.01% because first 8° bend will be used to determine the beam energy. Emittance growth due to dispersion mismatch at injection is proportional to $(\Delta p/p)^2$. It is negligible in our case because the acceptable $\Delta p/p$ is 1×10^{-4} to maximize capture in the LEB. Nominal values of η and η' are zero at injection.

The quadrupole magnet power supplies have been specified to have a stability of 0.1% of the full scale current. With this range of error, we used a slightly modified TRANSPORT code to simulate 250 beamlines corresponding to different sets of random errors on the quadrupole fields. Each set of errors produces β mismatch at injection, from which the emittance dilution factor is obtained [4]. These factors are plotted in figure 4 for 100 sets only for clarity. Emittance growth is unacceptable in the high β mode, in which the β function in x-plane near the dipole magnets is about 520 m. Elsewhere in the line, it does not exceed 125 m. This mode is necessary for accurate definition and determination of the momentum spread. Major contribution to the emittance growth comes from the field errors in quadrupoles Q3 and Q4. Figure 4 also shows the dilution factors for a low β mode in which the maximum β is about 130 m. This mode is quite satisfactory for LEB injection and the emittance growth is below 5% in 95% of the cases studied.

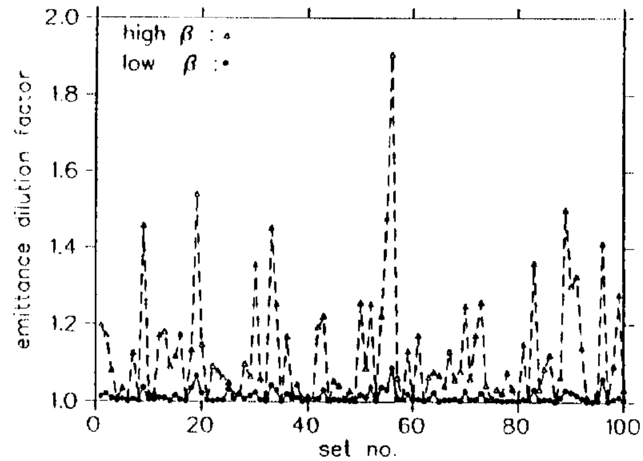

Figure 4. Emittance dilution factors due to quadrupole power supplies' instability of 0.1% of full scale current.

Stripper foil is the single largest source of emittance growth. Initial calculations have been done using the multiple scattering and the plural scattering models. Foil thickness is determined by the desired stripping efficiency. Ideally, all the incoming H^- should be stripped to H^+. The number of beam traversals through the foil during injection process should be minimized. This requirement can be translated into the rate at which the bump field is withdrawn. We have specified [5] that the bump field should fall to 87% of its peak value in 10.8 μs in the Collider filling mode (3 turn injection). In this time interval, physical center of the linac bunch just clears the inner edge of the foil, which is 12 mm wide to intercept, fully, the incident beam. A power supply with such a requirement is difficult but feasible to make. The expected emittance growth is 0.06 π mm-mrad, rms, normalized, as per the multiple scattering model for a lattice β=14.7 m at the foil. The plural scattering model, however, predicts a lower emittance growth, by a factor of almost 2, for the same foil thickness. Foil thickness will be optimized experimentally during the LEB commissioning.

IV. SUMMARY

The Linac to LEB transfer line meets all the requirements for good injection including control of the emittance growth. It will be easy to tune and offers ion optical flexibility.

V. ACKNOWLEDGEMENTS

We thank Warren Funk for many useful discussions and suggestions on almost all the aspects of this line. Several staff of the Accelerator Systems Division, SSCL, are contributing to the construction of this line. Our thanks to all of them.

IV. REFERENCES

[1] R. K. Bhandari, E. Seppi and S. Penner, "Design Characteristics of the Linac-LEB Transfer Line for the SSC," Record of the 1991 Particle Accelerator Conference, Vol. 1, pp. 351-354.

[2] L. Funk, "The SSC Linear Accelerator," these proceedings.

[3] S. Penner, "Injection-By-Stripping Loss Effects," SSCL Internal Note, ADOD-008L February 4, 1991.

[4] M. Syphers, "Injection Mismatch and Phase Space Dilution," Fermilab Note, FN-458, June 1987.

[5] S. Penner, "Conceptual Design of the LEB Injection Girder," SSCL Internal Note, ADOD-019L, April 25, 1991.